Lyapunov-exponent spectra for the Lorenz model

Jan Frøyland and Knut H. Alfsen
Institute of Physics, University of Oslo, Oslo 3, Norway
(Received 30 June 1983)

Using a fast algorithm we have calculated the Lyapunov exponents at about 6000 parameter points in the range $0.1 < r < 520$, $\sigma = 10$, and $b = \frac{8}{3}$ of the Lorenz model. In the chaotic region we find a large number of narrow windows containing periodic orbits—somewhat similar to what is the case in the one-dimensional logistic map.

I. INTRODUCTION

The interest in nonlinear dynamical systems has rapidly increased over the last few years, and a large number of more or less physically realistic models have appeared. A common feature of these models is the stochastic, or chaotic, behavior they show for certain ranges of parameters governing the systems. This behavior is now understood to be due to the presence of so-called "strange attractors."[1,2] For the description of a model it is of great importance to be able to describe the regions in parameter space where strange attractors are expected to appear in the system. Also, in systems where chaotic behavior seems to dominate, narrow regions with ordered periodic orbits may exist. The existence and positions of these "windows" are also important to ascertain.

One of the most powerful tools in this respect is the study of the asymptotic divergence or convergence of nearby orbits in the system. The behavior of these orbits are, in turn, characterized by their Lyapunov exponents. (See, for instance, Ref. 3 and references therein.) Numerical methods for calculating these exponents have been given by Benettin, Galgani, Georgielli, and Strelcyn[4,5] and by Shimada and Nagashima.[3] Unfortunately, the need for frequent coordinate changes makes these methods rather inefficient. However, recently one of us[6] has proposed an algorithm that apparently is much faster than existing ones, at least for low-dimensional systems. The main purpose of this paper is to demonstrate the use of this method. We do this by investigating the behavior of the Lorenz model,[7] as one of the controlling parameters is varied in a systematic manner. The Lyapunov exponents are found to be a practical tool in discussing the phenomena of bifurcations and in finding periodic orbits.

The number of papers dedicated to the study of the Lorenz model is truly astonishing. (The book by Sparrow[8] contains an extensive bibliography.) In spite of this large effort, however, our investigation reveals that there are still basic properties of the model left to be discovered and studied.

II. ALGORITHM

The theoretical basis for the calculations performed in this study is given in Ref. 6, but for the sake of completeness we shall here repeat the main results.

Let $\vec{D}^{(k)}(t)$ be an $\binom{n}{k}$-dimensional vector satisfying

$$\dot{\vec{D}}^{(k)}(t) = M^{(k)}[\vec{x}(t)]\vec{D}^{(k)}(t) \ , \tag{1}$$

where $\vec{D}^{(k)}(0)$ are arbitrary nonzero initial states and $M^{(k)}$ are n matrices defined in Ref. 6. By integrating this system of equations along with the orbit and forming

$$S^{(k)}(t) = \sum_{i=1}^{\binom{n}{k}} D_i^{(k)}(t) \ , \tag{2}$$

one can show that the Lyapunov exponents are given by

$$l^{(k)} = \lim_{t\to\infty} \left[\frac{1}{t} \ln |S^{(k)}(t)/S^{(k-1)}(t)| \right] \ . \tag{3}$$

Under- and overflow problems are easily taken care of by using the scaling properties of Eq. (1).

As was shown in Ref. 4 and recently in Ref. 9, at least one of the Lyapunov exponents vanishes exactly, unless the orbit ends on a fixed point. This property of the exponents serves as as useful check on the accuracy of the numerical calculations.

III. LORENZ MODEL

The set of three real, first-order differential equations describing the Lorenz model are[7]

$$\begin{aligned} \dot{x} &= -\sigma x + \sigma y \ , \\ \dot{y} &= -xz + rx - y \ , \\ \dot{z} &= xy - bz \ , \end{aligned} \tag{4}$$

where σ, b, and r are real parameters. The $M^{(k)}$ matrices associated with Eqs. (4) are

$$M^{(1)} = \begin{pmatrix} -\sigma & \sigma & 0 \\ -z+r & -1 & -x \\ y & x & -b \end{pmatrix} \ , \tag{5a}$$

$$M^{(2)} = \begin{pmatrix} -1-b & z-r & -y \\ -\sigma & -\sigma-b & -x \\ 0 & x & -1-\sigma \end{pmatrix} \ , \tag{5b}$$

and

$$M^{(3)} = -1-\sigma-b \ . \tag{5c}$$

Since $M^{(3)}$, the trace of the Jacobian, is constant, it follows[3] that

$$\sum_{k=1}^{3} l^{(k)} = -1-\sigma-b \ , \tag{6}$$

independent of the orbit. This constitutes another check on

the numerical accuracy of the algorithm used. This also implies the interesting result

$$-\tfrac{1}{2}(1+\sigma+b) \leq l^{(2)} \leq 0 \ . \tag{7}$$

The lower limit is realized when $l^{(2)}=l^{(3)}$ (and, hence, $l^{(1)}=0$). As we shall show in Sec. IV this may happen over an interval in parameter space, not just at isolated points. In general, this occurs for Lyapunov exponents associated with a complex conjugate set of eigenvalues of the Jacobian matrix. This kind of phenomenon is also observed in other systems, e.g., the Henon map.[10]

It has become customary in studying the Lorenz model to keep the parameters σ and b fixed while considering the "Reynolds number" r as the controlling parameter. The characteristic behavior of the system as r is varied can then be roughly summarized as follows: For $0<r<1$ there is one fixed point $O=(0,0,0)$ and it is stable. When r increases above 1 this becomes an unstable saddle point while two new stable fixed points appear at

$$C_{\pm}=[\pm\sqrt{b(r-1)},\ \pm\sqrt{b(r-1)},\ r-1] \ .$$

These are stable for $r<r_c$ (assuming $\sigma>b+1$), where $r_c=\sigma(\sigma+b+3)/(\sigma-b-1)$. At this point an inverse Hopf bifurcation takes place and chaotic behavior, due to the appearance of a strange attractor, is observed. However, for $r_s<r<r_c$, where $r_s\approx 24.06$, chaos and fixed points may coexist.[11–13] In the chaotic range $r_c<r$, several periodic windows have been discovered and studied,[13–15] and the Feigenbaum-type period doubling sequences of bifurcations[16] have been identified for decreasing values of r, together with symmetry-breaking bifurcations. Also, inverse bifurcations have been observed in the chaotic region.[17] For very large values of r, approximate, analytic, periodic solutions have been obtained in Ref. 18.

We note that Eqs. (4) are invariant under the transformation $x\rightarrow -x$, $y\rightarrow -y$, $z\rightarrow z$ (reflection about the z axis). For a stable periodic orbit this implies that either the orbit will transform into itself—this will be called a symmetric orbit, or it will transform into a new stable and periodic orbit—this will be called an asymmetric orbit.

IV. RESULTS AND DISCUSSION

We have calculated the three Lyapunov exponents of the Lorenz model for fixed "canonical" parameter values $\sigma=10$ and $b=\frac{8}{3}$, varying r in steps of $\Delta r=0.1$ in the range $0.1\leq r\leq 520$. We have employed the algorithm briefly outlined in Sec. II together with a standard fourth-order Runge-Kutta integration scheme. The step length used in the intergration was $\Delta t=0.01$ throughout, which for our purposes gave sufficiently accurate results. However, we noted occurrences of spurious dips in the Lyapunov exponents near points where very fine details of the orbit are important, i.e., accumulation points of the period doubling bifurcation series. These dips disappeared when Δt was diminished to 0.001.

The main result is displayed in Fig. 1, where the Lyapunov exponents ($l^{(k)}$, $k=1,2,3$) are shown versus r. We started the calculation at the highest-r value ($r=520$) and with an initial position in the vicinity of one of the unstable fixed points. After a suitable transition time, $t=50$, the integration of Eq. (1) was started and carried on for an additional time $t=400$. The Lyapunov exponents were then calculated from Eq. (3) and r was decreased by $\Delta r=0.1$. The integration at the new r value was started at the last obtained position on the orbit at the previous r. This reduced the time necessary for transients to die out. This procedure was continued down to $r\approx 24.0$, which is somewhat below the critical value $r_c=24.74$ for this system. For values below $r\approx 24.0$ we used the fixed points $C_{\pm}$ as the orbit. This resulted in a small jump in $l^{(2)}$ at the transition point.

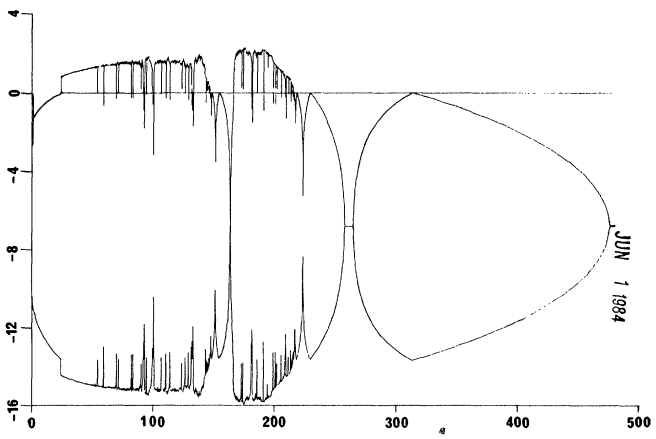

FIG. 1. Three Lyapunov exponents in the range $0.1<r<520.0$. Intervals between points are $\Delta r=0.1$. Neighboring points have been joined by a straight line to guide the eye.

For $r>24.74$ either $l^{(1)}$ or $l^{(2)}$ must vanish[3,9] and this is clearly shown in Fig. 1. Furthermore, for our choice of parameters, $l^{(2)}$ is limited to the range $-6.833\leq l^{(2)}\leq 0$ [cf. Eq. (7)]. Hence $l^{(3)}$ may be obtained from $l^{(1)}+l^{(2)}$ when $r\geq 24.06$ by a trivial reflection about the line $l=-6.8333$. Nevertheless, we have displayed all three Lyapunov exponents in Fig. 1. This is done in order to emphasize the cause of the flat bottoms of some of the dips, and the flat region starting at $r\approx 475$, and apparently continuing forever. In fact, although hardly visible on the scale of Fig. 1, the dip near $r\approx 163.5$ has a flat interval of finite length at the bottom. Perhaps the most striking feature of Fig. 1 is the large number of periodic "windows," i.e., regions where $l^{(1)}=0$, while $l^{(2)}$ and $l^{(3)}<0$. The most prominent ones, largely described in the literature already,[14,15,17] are found at r values in the vicinity of 150–167, 133, 100, and 93, but, in addition, there is a large number of narrower windows seen as vertical lines in the figure. Furthermore, by decreasing the step length in r, numerous other windows become visible. We shall return to this point later.

Figure 1 should be closely compared with Fig. 2, which is a quasi-Poincaré plot generated by plotting the distance between the origin and the intersection point between the orbit projection into the x-y plane and the line $x=y$ vs r. By doing so we identify points in the first and third quadrant in the $x-y$ plane, and hence do not distinguish between orbits of opposite symmetry. In other words, one includes automatically points from orbits that may be reached by the transformation $x\rightarrow -x$, $y\rightarrow -y$, $z\rightarrow z$. For chaotic orbits, 300 points have been plotted for r values separated by $\Delta r=0.67$. As one can see from a comparison

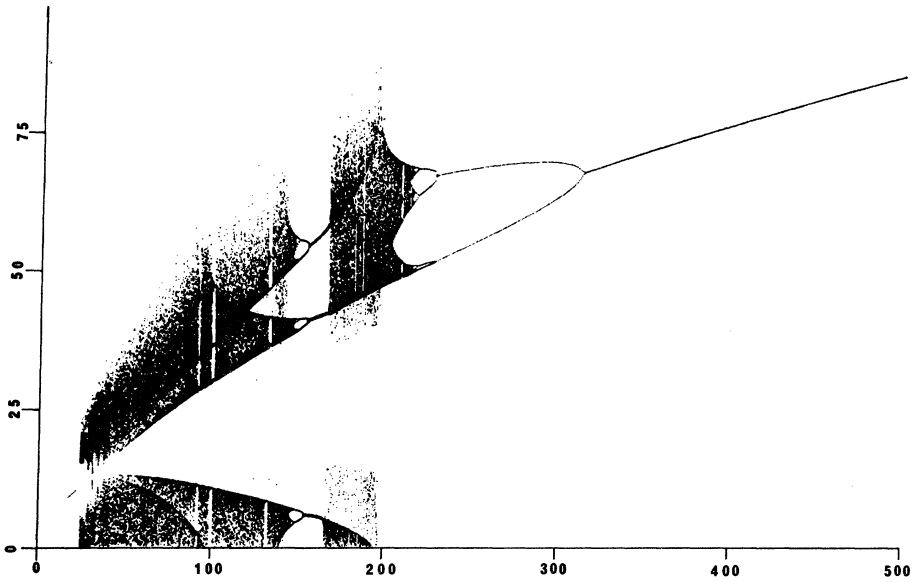

FIG. 2. Quasi-Poincaré plot (see Sec. IV) in the range $24 < r < 520$. At each r value 300 points have been plotted. Intervals in r are $\Delta r = 0.67$.

with Fig. 1, the Lyapunov exponents behave as expected in that the periodic orbits bifurcate whenever $l^{(2)}$ hits zero, while $l^{(1)} > 0$ signals chaotic orbits.

Starting from the highest-r value, the first bifurcation occurs at $r \approx 313$. This is not a period doubling bifurcation, but a bifurcation that destroys the symmetry of the periodic orbit.[3] Near this bifurcation the plot in Fig. 2 looks deceptively normal, but in fact, the two prongs emerging from one bifurcation point belong to two different orbits with opposite symmetry. Thus, from $r \approx 313$ and down to the band merging point at $r \approx 205$, there are at least two separate basins of attraction. The bifurcation sequence following the symmetry-breaking bifurcation at $r \approx 313$ is of the normal period doubling type with an accumulation point at[17] $r \approx 215.364$. The observed convergence rates apparently agree with the asymptotic value $\delta = 4.669\,20\ldots$ expected from universality.[16] This type of behavior has also been observed in other periodic windows, and is probably a characteristic of all of them. Figure 2 has many additional features in common with, or reminiscent of, similar plots for the one-dimensional logistic map.[19] Notably, we find sharply defined dark bands crisscrossing the plot in both cases. One can even see regions similar to the "crisis" regions.[20] However, the details are different. For instance, the upper edge of the plot in Fig. 2 is poorly defined for $r \lesssim 197$ (i.e., after the appearance of the crisis regions). In contrast to the upper edge, the lower edges in Fig. 2 seem to be sharply defined down to some r value where also these boundaries become fuzzy. We have magnified the relevant region plotting up to 600 points at each r value, but the qualitative picture does not change.

A periodic orbit may be characterized (not necessarily uniquely) by its winding numbers in the x-y plane around the three unstable fixed points C_-, O, and C_+. In order to study the positions of a few of the windows in r space, we have focused our attention on symmetric orbits with winding numbers of the form $(n,1,n)$, where n is a positive integer and 1 is the winding number around the origin. We have also studied asymmetric orbits with winding numbers $(1,1,n)$. Projections of the symmetric orbits are shown in Fig. 3 for $n = 1$–7. The corresponding r values for the approximate positions of the minimum values of the second Lyapunov exponent are listed in Table I for both symmetric and asymmetric orbits. The position in r space of these periodic orbits are found to follow the relation

$$r_n = r_\infty \exp[c/(n+d)] \tag{8}$$

very closely. In Eq. (8), r_∞, c, and d are constants, while n

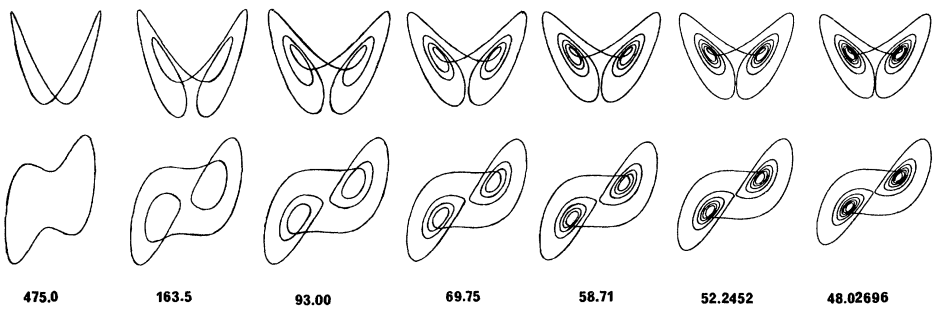

FIG. 3. Projections into the z-x plane (upper row) and the y-x plane (lower row) of the symmetric orbits of the type $(n,1,n)$ (see Sec. IV). The scales are arbitrary and special in each case.

TABLE I. Approximate positions of the local minima of $l^{(2)}$ for symmetric orbits of the form $(n,1,n)$ and asymmetric orbits of the form $(1,1,n)$.

n	Symmetric $(n,1,n)$	Asymmetric $(1,1,n)$
1	475.0	262.0
2	163.67	100.55
3	93.015	71.5
4	69.7436	59.25
5	58.7120	52.4544
6	52.2452	
7	48.026 96	

is the winding number defined previously. In the symmetric case a good fit is obtained with $r_\infty = 28.55$, while in the asymmetric case $r_\infty \approx 30$. The main purpose of these fits was to use them to predict the position of the next r_n in the series. Taken at face value, Eq. (8) would suggest the existence of accumulation points, but we have reasons to believe that such accumulation points do not exist for $b = \frac{8}{3}$.

A noteworthy difference between the logistic map and the Lorenz model is illustrated in Fig. 4, where we have displayed the two largest Lyapunov exponents in the very narrow window $48.0253 > r > 48.0272$ associated with the (7,1,7) symmetric orbit. The similarity between this and other, much wider windows (Fig. 1) is amazing. Notice that $l^{(1)}$ apparently goes smoothly to zero as the window is approached from below, while there is a finite jump at the high-r end of the window. Provided this last phenomenon is genuine, it is in contrast to the one-dimensional case where this type of transition probably has a critical exponent[21] of $\frac{1}{2}$. The jump in the highest Lyapunov exponent may be due to bistability of the system which precludes an intermittent behavior just above the window. This is in contrast to what has been found for higher values of r.[22]

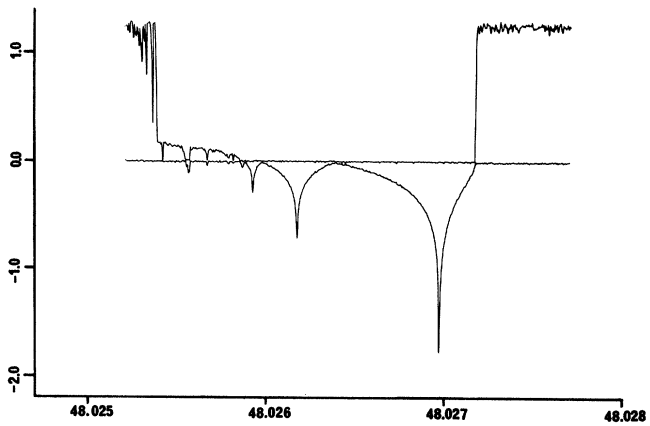

FIG. 4. Two largest Lyapunov exponents in the interval $48.0252 < r < 48.0276$. Intervals in r are $\Delta r = 0.000\,05$. Neighboring points have been joined by a straight line.

However, our conclusion is uncertain due to the relatively short orbits we have used.

The last autonomous periodic orbit found by us is the (7,1,7) symmetric orbit which is maximally stable at $r_7 = 48.026\,96 \pm 0.000\,02$. With the use of Eq. (8) to extrapolate to $n = 8$ gives $45.05 \lesssim r_8 \lesssim 45.10$. We have searched this region without finding any new window. This, of course, does not exclude that it is there. It may have been overlooked for a number of reasons: The step length in time and/or r may have been too large, the transition time allowed at the beginning of each calculation may have been too short, or we may have been outside the relevant basin of attraction.

All calculations were carried out in double precision on the 32-bit computer NORD-500. One of us (J.F.) is grateful for the financial support from the Norwegian Council for Sciences and the Humanities.

[1]D. Ruelle and F. Takens, Commun. Math. Phys. 20, 167 (1971).
[2]E. Ott, Rev. Mod. Phys. 53, 655 (1981); R. Shaw, Z. Naturforsch. 36A, 80 (1981).
[3]I. Shimada and T. Nagashima, Prog. Theor. Phys. 61, 1605 (1979).
[4]G. Benettin, L. Galgani, and J.-M. Strelcyn, Phys. Rev. A 14, 2338 (1976).
[5]G. Benettin, L. Galgani, A. Georgielli, and J.-M. Strelcyn, Meccanica 15, 9 (1980).
[6]J. Frøyland, Phys. Lett. 97A, 8 (1983).
[7]E. N. Lorenz, J. Atmos. Sci. 20, 130 (1963).
[8]C. Sparrow, *The Lorenz Equations: Bifurcations, Chaos and Strange Attractors* (Springer-Verlag, New York, 1982).
[9]H. Haken, Phys. Lett. 94A, 71 (1983).
[10]S. D. Feit, Commun. Math. Phys. 61, 249 (1978).
[11]J. A. Yorke and E. D. Yorke, J. Stat. Phys. 21, 263 (1979).
[12]V. S. Afraimovich, V. V. Bykov and Shil'nikov, Dokl. Akad. Nauk SSSR 234, 336 (1977) [Sov. Phys. Dokl. 22, 253 (1977)].
[13]T. Shimizu and N. Morioka, Phys. Lett. 69A, 148 (1978).
[14]T. Shimizu and N. Morioka, Phys. Lett. 66A, 182 (1978).
[15]V. Franceschini, J. Stat. Phys. 22, 397 (1980).
[16]M. J. Feigenbaum, J. Stat. Phys. 19, 25 (1978).
[17]E. N. Lorenz, Ann. N.Y. Acad. Sci. 357, 282 (1980).
[18]K. A. Robbins, SIAM J. Appl. Math. 36, 457 (1979).
[19]P. Collet and J.-P. Eckman, *Iterated Maps on the Interval as Dynamical Systems,* edited by A. Jaffe and D. Ruelle, Progress in Physics, Vol. 1 (Birkhäuser, Boston, MA, 1980).
[20]C. Grebogi, E. Ott, and J. A. Yorke, Phys. Rev. Lett. 48, 1507 (1982).
[21]J. E. Hirsch, B. A. Huberman, and D. J. Scalapino, Phys. Rev. A 25, 519 (1982).
[22]P. Manneville and Y. Pomeau, Phys. Lett. 75A, 1 (1979).